Candle soot nanoparticles-polydimethylsiloxane composites for laser ultrasound transducers

Wei-Yi Chang,[1] Wenbin Huang,[1,2] Jinwook Kim,[1] Sibo Li,[1] and Xiaoning Jiang[1,a)]
[1]*Department of Mechanical and Aerospace Engineering, North Carolina State University, Raleigh, North Carolina 27695, USA*
[2]*The State Key Laboratory of Mechanical Transmission, Chongqing University, Chongqing 400044, China*

(Received 1 July 2015; accepted 3 October 2015; published online 23 October 2015)

Generation of high power laser ultrasound strongly demands the advanced materials with efficient laser energy absorption, fast thermal diffusion, and large thermoelastic expansion capabilities. In this study, candle soot nanoparticles-polydimethylsiloxane (CSNPs-PDMS) composite was investigated as the functional layer for an optoacoustic transducer with high-energy conversion efficiency. The mean diameter of the collected candle soot carbon nanoparticles is about 45 nm, and the light absorption ratio at 532 nm wavelength is up to 96.24%. The prototyped CSNPs-PDMS nano-composite laser ultrasound transducer was characterized and compared with transducers using Cr-PDMS, carbon black (CB)-PDMS, and carbon nano-fiber (CNFs)-PDMS composites, respectively. Energy conversion coefficient and −6 dB frequency bandwidth of the CSNPs-PDMS composite laser ultrasound transducer were measured to be 4.41×10^{-3} and 21 MHz, respectively. The unprecedented laser ultrasound transduction performance using CSNPs-PDMS nano-composites is promising for a broad range of ultrasound therapy applications. © *2015 AIP Publishing LLC*. [http://dx.doi.org/10.1063/1.4934587]

Ultrasound transducers with high intensity or high peak pressure can be used in a broad range of biomedical ultrasound therapy and drug delivery applications.[1,2] Optoacoustic transducers are attractive because of their high power density, high frequency, and broad bandwidth. Furthermore, laser generated ultrasound offers an easy and efficient way to transform laser energy into short acoustic pulses without direct interaction between the laser and the subjects. Instead, a laser ultrasound transduction structure, usually consists of a laser light absorption layer and an thermal expansion layer.[3,4] In order to obtain high performance laser ultrasound transducers, active research has been focused on the absorbing materials such as carbon black (CB), carbon nanotubes (CNT),[4] graphite, metallic films,[5] gold nano-structures,[6,7] and gold nano-particles.[8] These single phase materials are known with high light absorption ratio, and thus, high temperature can be generated locally under laser exposure. Owing to their nanometer spatial configuration, thermal energy can be transferred into the expanding layer or matrix with high efficiency. Moreover, the thermal expanding material with a high thermal expansion coefficient is greatly demanded to achieve a high pressure acoustic pulse. Polydimethylsiloxane (PDMS) has been widely used as a thermal expanding layer because of its high thermal coefficient of volume expansion ($\alpha = 0.92 \times 10^{-3}\ K^{-1}$), which is much higher than water, tissue, ceramics, and metals.[9] As an example, Buma *et al*. proved that the conversion efficiency of thermoelastic effect was improved over 20 dB by using PDMS film instead of metallic film.[10]

In addition to a single phase light absorption layer and thermal expansion layer configurations, the composite materials capable of both light absorption and expanding have also been studied. Flat composite films with graphene and carbon nanotube showed the capability of generating high acoustic pressure over 7.5 MPa near the transducer surface under a laser input of 43.28 mJ/cm^2.[11] By employing the PDMS/gold nanoparticle nanocomposite, the laser ultrasound transduction efficiency was increased by 3 orders of magnitude compared with the aluminum thin film.[12] Baac *et al*. claimed that the CNT-PDMS composite-based laser ultrasound transducer generated strong optoacoustic pressure compared to metal composites.[4] Hsieh *et al*. reported an optoacoustic energy conversion efficiency of 15.6×10^{-3} Pa/(W/m^2) in a carbon nano-fiber (CNFs)-PDMS composite, which is much higher than that of the carbon black composite.[13] However, the current fabrication process for the absorbing layer preparation not only lacks precise dimension control but also is complicated, expensive, and less scalable.

Candle soot (CS) is a simple process for fabrication of carbon nanoparticles and has been attracting increasing attention in applications such as optoelectronic device and bioimaging.[14,15] Most of published works are focused on the special porous soot nanostructures,[16,17] because of the fact that hierarchical nanostructure nature of a CS layer has unique properties such as superhydrophobicity and high light absorption efficiency. For example, a 3-μm-thick super-amphiphobic surface coating of CS was used to reduce the light transmission to be less than 10% compared to a pristine glass for wavelengths above 500 nm. Each CS nano-particle is about 30–40 nm in diameter.[15] Moreover, candle soot nano-particles (CSNPs) can be deposited on substrates with any size and shape. In this paper, we demonstrate the potential of an optoacoustic transducer using CSNPs-PDMS nanocomposite in the generation of high frequency, broadband and high-energy intensity acoustic signal. The CSNPs-PDMS nanocomposite laser ultrasound transducers were

a)Electronic mail: xjiang5@ncsu.edu

prototyped, characterized, and compared with the Cr-, CB-, and CNFs-PDMS composite transducers, respectively.

First, a candle (diameter: 25 mm) with the paraffin wax as the main component was used to produce CSNPs at room temperature using a process called flame synthesis.[16] When the candle flame became stable, a total flame height of about 3 cm could be obtained. A glass slide was then mounted within the flame core at ~2 cm above the wick. After the 30 s growth process, this first glass slide was coated with a uniform CSNPs layer. Upon the CSNPs fabrication, a CSNPs-PDMS nanocomposite fabrication process was next developed (Fig. 1). The second glass slide was treated with silane coating for 6 h to become anti-adhesive. The PDMS base and curing agent (Sylgard 184) were mixed at a ratio of 10:1 and then placed in a vacuum chamber to degas for 30 min. The mixture was then poured onto the anti-adhesive glass slide, followed by a spin coating at 3000 rpm. Further, the 1st glass slide was placed on the anti-adhesive glass slide (or the 2nd slide), with the CSNPs layer on the 1st glass facing to the procured PDMS layer on the 2nd glass. Owing to the porous structure of the CSNPs layer, precured PDMS penetrated into the CS layer, forming the CSNPs-PDMS composite between the two glass slides. After the PDMS was fully cured at 65 °C for 1 h, the anti-adhesive glass slide was removed, and the CSNPs-PDMS composite remained on the 1st glass slide. Similarly, for the fabrication of CNFs-PDMS composite, a 25 μm thick CNFs layer consisting of fibers with an average diameter of 132.7 nm was used. The electrospinning preparation method of CNFs was reported in our previous paper.[13] The total thickness of the CNFs-PDMS composite was 57.8 μm. The CB-PDMS composite consisting of CB powder mixed with the PDMS solution was also prepared. As aggregations of CB could cause curing issue for PDMS, the concentration of CB was controlled to be 61.28% (% w/w).[13] The total thickness of CB-PDMS was 30 μm. The mixture ratio and curing conditions of PDMS were identical across the preparations for these three composites. For comparison, a metal control sample was fabricated by depositing a 100 nm Cr layer onto a glass slide followed by the spin coating of PDMS at 3000 rpm.

The morphology and structure of CSNPs were studied by using an emission scanning electron microscopy (SEM, FEI Verios 460L, OR), as shown in Figs. 2(a) and 2(b). The CSNPs are homogeneous, and the particle size is uniform with a diameter of around 45 ± 5 nm, forming a loose and branch-like network. After precured PDMS was transferred to CSNPs coated glass slide and cured, CSNPs became fully covered by PDMS and the arborized structure can be observed in Fig. 2(c). Compared with spin coating, a more gentle technique, i.e., direct transfer here, should be employed, which otherwise would wash away the loose CSNPs structure. The thickness of the CSNPs + PDMS and PDMS layers is 5.99 ± 0.5 μm and 18.44 ± 1.3 μm, respectively. It is more clearly observed that CSNPs are embedded in the PDMS layer, as shown in Figs. 2(d) and 2(e). The surface roughness of CSNPs was measured to be about 200 nm by a scanning probe microscopy (Dimension Icon, Bruker, Santa Barbara, CA).

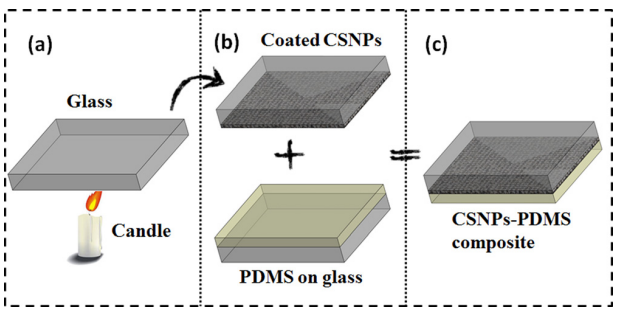

FIG. 1. Schematic diagram of the fabrication of CSNPs-PDMS composite.

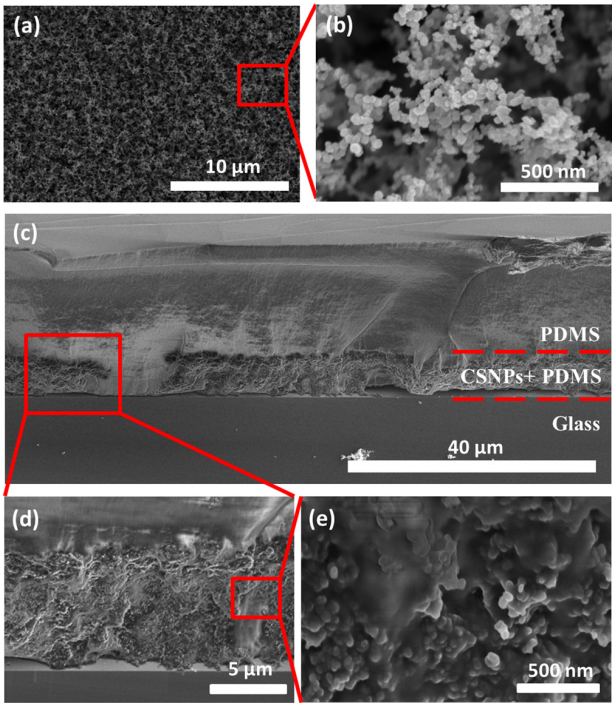

FIG. 2. (a) Low- and (b) high-resolution SEM images of CSNPs grown on glass. (c) Cross section of CSNPs-PDMS composite, and the thickness of PDMS is 18.44 ± 1.3 μm. (d) The thickness of CSNPs-PDMS is 5.99 ± 0.5 μm, (e) CSNPs are well embedded in PDMS.

Before the laser ultrasound characterizations, the optical properties of each composite were measured, including the optical reflection, transmission, and absorption coefficients. These optical properties were measured using a spectrometer (Agilent Cary 5000 UV-VIS-NIR, Santa Clara) with the measured area of 10 mm^2. The optical transmission and reflection coefficients of the CSNPs-PDMS composite were 0.015% and 3.659%, respectively. The optical absorption coefficient was 96.24 ± 0.31% by averaging the measurements at different spots on 20 mm × 25 mm samples. The small variance implied that the optical absorption coefficient across the film surface is macroscopically homogeneous. The absorption coefficients of the CNFs- and CB-PDMS composites were measured to be 95 ± 0.72% and 95.85 ± 0.22%, respectively. These carbon nanocomposites all present excellent light absorption properties, similar to the previous studies.[18] Among these three composites, the CSNPs-PDMS composite exhibits the lowest laser reflection coefficient and the highest absorption coefficient, which is

largely due to the unique hierarchical and arborized structure of CSNPs.[19]

The prepared laser transducer prototypes were characterized using the experimental setup shown in Fig. 3(a). The excitation laser source is a 532 nm Q-switched Nd:YAG pulsed laser (SL-III-10, Continuum, San Jose, CA) with a pulse duration of 6 ns and a 10 Hz repetition rate. The laser beam size is about 10 mm in diameter. The laser energy was measured by a pyroelectric energy sensor (J-50MB-YAG, Coherent, Portland, OR). The laser beam penetrated through water for a distance of 5 mm and then reached the nanocomposite. A high-frequency hydrophone (HGL-0085, ONDA Corp., Sunnyvale, CA) was utilized as a receiver to detect the ultrasound signals generated by the composite. The hydrophone we used has an aperture size of 200 μm, which is much smaller than the size of the transducer. A 4.2 mm distance between the nanocomposite and the hydrophone was chosen to satisfy a plane wave configuration.[20] The trigger signal was provided by the laser source. The received hydrophone signal was amplified by a preamplifier (20 dB) and then recorded by a digital oscilloscope (DSO7104B, Agilent, Santa Clara, CA). Each waveform was obtained by averaging 16 signal traces in time domain.

Under the same laser energy density with a moderate value of 3.57 mJ/cm^2, the generated acoustic signals from four transducers were plotted in Fig. 3(b). The largest acoustic pressure from the CS-PDMS composite could reach 4.8 MPa, which is twice that of CNFs-PDMS, six times of CB-PDMS, and sixteen times of the Cr-PDMS composite signal. The measured pressure from CSNPs-PDMS reached half of the maximum achievable pressure of the PDMS based transducers predicted by the theory under an ideal assumption.[21] The following discussions are only focused on the three carbon based composites. The efficiency of the photoacoustic wave generation can be described by the following equation:

$$\eta = \frac{E_a}{E_{optical}}, \tag{1}$$

where $E_{optical}$ is the energy of the laser pulse and E_a is the energy of the acoustic signal. E_a can be estimated by the following expression:

$$E_a = \frac{1}{\rho c} A \int_0^\infty p^2(t) dt, \tag{2}$$

where ρ and c are the density and sound velocity of water, respectively. p is the acoustic pressure, which was measured as shown in Fig. 3(b). A is the acoustic spot area and approximately has the same size of the laser beam near the transducer surface where our hydrophone was placed. The laser energy can be calculated to be 2.8 mJ. The ultrasound energy obtained from the CSNPs-PDMS, CNFs-PDMS, and CB-PDMS composites can be estimated to be 12.3 μJ, 4.65 μJ, and 0.95 μJ, respectively, via Eq. (2). Hence, the energy conversion efficiency can be obtained as 4.41×10^{-3}, 1.66×10^{-3}, and 0.34×10^{-3}, respectively. The energy conversion efficiency of the CSNPs-PDMS composite is higher than the reported valued for gold nanoparticles composite (0.18×10^{-3})[22] and carbon nanotube composite (1.4×10^{-3}).[9] It is noted that the latter transducer adopted a concave lens to focus the acoustic beam, and the acoustic energy calculation assumed an even acoustic pressure distribution with the amplitude equal to the measured pressure at the focal spot. This could render an overestimation of the acoustic energy and indicates a smaller conversion efficiency

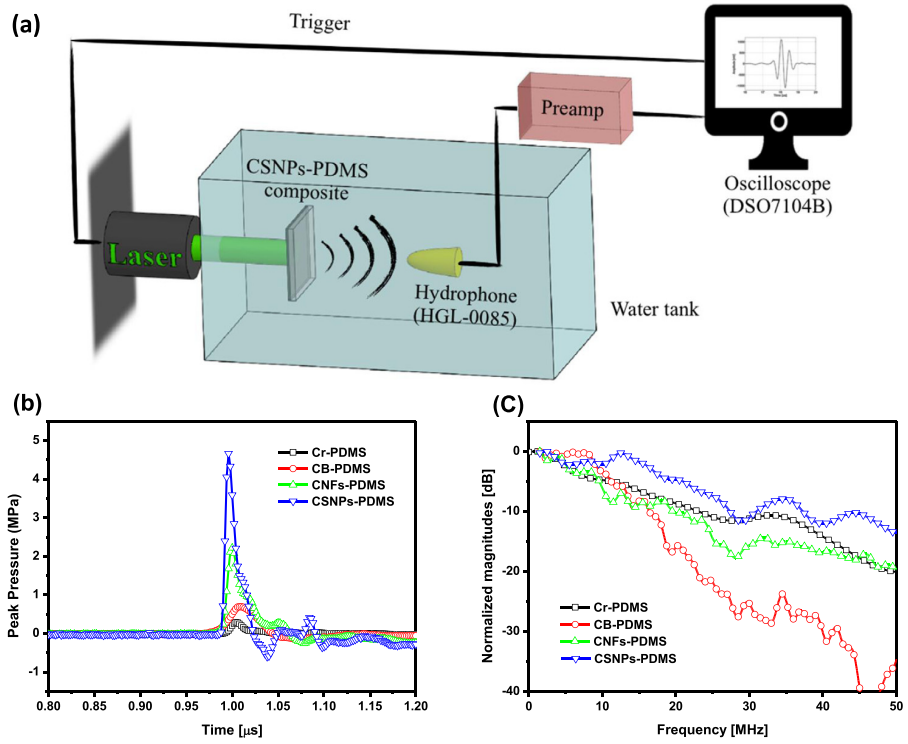

FIG. 3. (a) Experimental setup for laser ultrasound generation and characterization. (b) Optoacoustic signals of laser generated ultrasound waveform from CSNPs-, CNFs-, and CB-PDMS film. (c) Frequency spectrum from CSNPs-, CNFs-, and CB-PDMS film.

than the reported value. Therefore, the unprecedented high energy conversion efficiency was obtained from the CSNPs-PDMS composite laser transducer reported in this letter.

The superior performance of the CSNPs-PDMS composite can be explained by its spatial configuration in nanoscale. The amplitude of the photoacoustic signal for a small source at nanosecond time scales is related to the temporal temperature gradient generated in the PDMS by the heat diffusion from the CNPs.[19,23] A low interfacial thermal resistance leads to a fast heat transfer and a temperature profile that closely resembles the profile of the laser pulse and shows the stronger photoacoustic signal. In contrast, the higher interfacial thermal resistance would increase the nanoparticle temperature but decrease the rate of heat release into the adjacent medium (PDMS). Among these three types of composite, the absorber in CSNPs-PDMS possesses the largest surface to volume ratio due to the three dimensional nano-sizes of CSNPs; therefore, a relative larger passageway is available for dissipating heat into PDMS given the same volume ratio of the absorber to the PDMS matrix among various composites. CNFs exhibit nanosizes in two dimensions vertical to the fiber growth orientation; thus, energy could be radically transferred into PDMS with high efficiency. However, the contact area with PDMS is smaller than that of CSNPs, leading to a higher thermal resistance and thus a lower photoacoustic conversion efficiency.[21]

As shown in Fig. 3(c), the measured center frequency and −6 dB bandwidth of the laser ultrasound induced by the CSNPs-PDMS composite was 10 MHz and 21 MHz, respectively. The acoustic signal generated by the CNFs-PDMS composite displays a similar frequency profile with CSNPs-PDMS, although they have different thicknesses. This matches with the reported experimental and theoretical results which indicates that the frequency spectrum of the acoustic signal is mainly determined by the temporal profile of laser pulse given a proper range of the composite thickness.[24] Also, the differences in energy conversion efficiency of the three composites studied here are only related with the absorption and heat dissipation capabilities of the functional materials, instead of the thickness variation, given that the composite thickness is much larger than the optical penetration depth while thin enough to prohibit great attenuation of high frequency signals over a long distance. Intriguingly, the bandwidth of CB-composite is much narrower than the CNFs and CSNPs composite (about 7.5 MHz), and the reason is believed to lie in the non-uniform mixing and dispersion of the CB particles in the PDMS matrix, leading to a large optical penetration depth.[21,25]

To further understand the optoacoustic ultrasound field generated by the CSNPs-PDMS film, the acoustic pressure was measured along the axial direction by varying the distance from 4.2 mm to 46.2 mm under a 3.57 mJ/cm^2 laser energy. Fig. 4(a) shows the maximum positive and negative pressures measured at each spot. The peak positive and negative pressures decreased at further distances. Moreover, to characterize the relationship between the acoustic pressure with the laser energy density, the laser energy density ramped from 3.57 mJ/cm^2 to 28.03 mJ/cm^2. This maximum laser energy density was chosen because it reaches the maximum capability of our equipment. In order to prohibit potential damage to the hydrophone when the laser energy insertion was high, it was placed at 46.2 mm, where the acoustic pressure is about five times lower than that near the surface. The results were plotted in Fig. 4(b), and the waveforms were shown in Figs. 4(c) and 4(d) in the temporal and frequency domains, respectively. The subsequent echoes

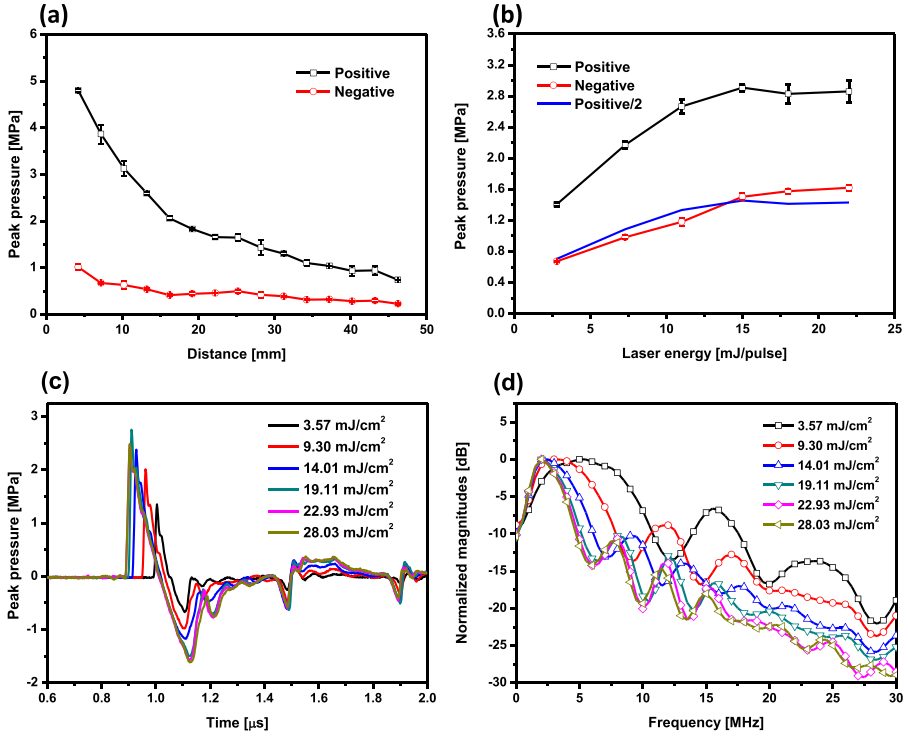

FIG. 4. (a) Distributions of the positive and negative ultrasound pressures along the axial direction generated by the CSNPs-PDMS film under a laser energy density of 3.57 mJ/cm^2. (b) Measured pressure amplitudes versus laser energy at the position of 46.2 mm to the transducer surface. (c) Acoustic signals from the CSNPs-PDMS film with different laser energy inputs from 3.57 mJ/cm^2 to 28.03 mJ/cm^2. (d) Waveforms shown in frequency domains.

arise from the reflection on the back surface of glass slide. The phase reverse is due to the impedance mismatch between the glass and water medium. The positive pressure was almost two times larger than the negative pressure, which was demonstrated by the well match between the line denoting half of the positive pressure and the negative pressure line.[26]

The positive peak values became saturated when the laser energy exceeded 22.93 mJ/cm^2. Similar phenomena have been reported by other researchers using carbon nanotube, and they attributed this effect to the bandwidth limit of the employed hydrophone.[9] However, here we suppose it to be caused by the partial detachment of the film from the glass slide. Small bumps have been observed to form under high laser energy insertion, with a vacuum or air environment inside. Owing to the low impedance of the air compared to that of the composite, acoustic wave will reverberate on the interface with a 180° phase change. Therefore, the reflective wave will sum together with the forward propagating wave with no time delay, resulting in the destructive interference, thus suppressing the total acoustic pressure. The methods to promote the adhesion between the substrate and the composite layer to withstand high intensity laser input are under investigation.

In conclusion, we demonstrated an optoacoustic transducer by using the CSNPs-PDMS composite. It is confirmed that candle soot nanoparticles can provide an efficient light absorption and heat transfer performance. With the excitation using a low laser energy density (3.57 mJ/cm^2), the CSNPs-PDMS composite laser transducer showed a high energy conversion coefficient (4.41×10^{-3}) at a broad frequency range (21 MHz) among the transducers using the CB-, CNFs-, and CSNPs-PDMS composites. In brief, a simple and non-expensive but reliable fabrication process has been demonstrated for developing advanced laser ultrasound transducers, which holds great potential for ultrasound based therapeutic applications.

The authors would like to acknowledge Dr. Tiegang Fang at NCSU for allowing us to use the Nd:YAG laser system. The authors would also like to acknowledge Dr. Chih-Hao Chang at NCSU for using the spectrometer. This work was partly supported by the Research Innovation Seed Funding project at NC State (Grant No. 762162).

[1]J. Hindley, W. M. Gedroyc, L. Regan, E. Stewart, C. Tempany, K. Hynnen, N. Macdanold, Y. Inbar, Y. Itzchak, and J. Rabinovici, Am. J. Roentgenol. **183**(6), 1713 (2004).
[2]S.-T. Kang and C.-K. Yeh, Langmuir **27**(21), 13183 (2011).
[3]Y. Hou, S. Ashkenazi, S.-W. Huang, and M. O'Donnell, IEEE Trans. Ultrason. Ferroelectr. Freq. Control **54**(3), 682 (2007).
[4]H. W. Baac, J. G. Ok, H. J. Park, T. Ling, S.-L. Chen, A. J. Hart, and L. J. Guo, Appl. Phys. Lett. **97**(23), 234104 (2010).
[5]E. Biagi, F. Margheri, and D. Menichelli, IEEE Trans. Ultrason. Ferroelectr. Freq. Control **48**(6), 1669 (2001).
[6]Y. Hou, J.-S. Kim, S. Ashkenazi, M. O'Donnell, and L. J. Guo, Appl. Phys. Lett. **89**(9), 093901 (2006).
[7]Y. Tian, N. Wu, X. Zou, H. Felemban, C. Cao, and X. Wang, Opt. Eng. **52**(6), 065005 (2013).
[8]Y. Tian, N. Wu, K. Sun, X. Zou, and X. Wang, J. Comput. Acoust. **21**(02), 1350002 (2013).
[9]H. W. Baac, J. G. Ok, A. Maxwell, K.-T. Lee, Y.-C. Chen, A. J. Hart, Z. Xu, E. Yoon, and L. J. Guo, Sci. Rep. **2**, 989 (2012).
[10]T. Buma, M. Spisar, and M. O'Donnell, Appl. Phys. Lett. **79**(4), 548 (2001).
[11]S. H. Lee, M.-A. Park, J. J. Yoh, H. Song, E. Y. Jang, Y. H. Kim, S. Kang, and Y. S. Yoon, Appl. Phys. Lett. **101**(24), 241909 (2012).
[12]N. Wu, Y. Tian, X. Zou, V. Silva, A. Chery, and X. Wang, J. Opt. Soc. Am. B **29**(8), 2016 (2012).
[13]B.-Y. Hsieh, J. Kim, J. Zhu, S. Li, X. Zhang, and X. Jiang, Appl. Phys. Lett. **106**(2), 021902 (2015).
[14]H. Liu, T. Ye, and C. Mao, Angew. Chem., Int. Ed. **46**(34), 6473 (2007).
[15]S.-T. Yang, L. Cao, P. G. Luo, F. Lu, X. Wang, H. Wang, M. J. Meziani, Y. Liu, G. Qi, and Y.-P. Sun, J. Am. Chem. Soc. **131**(32), 11308 (2009).
[16]L. Yuan, J. Dai, X. Fan, T. Song, Y. T. Tao, K. Wang, Z. Xu, J. Zhang, X. Bai, and P. Lu, ACS Nano **5**(5), 4007 (2011).
[17]X. Deng, L. Mammen, H.-J. Butt, and D. Vollmer, Science **335**(6064), 67 (2012).
[18]Z.-P. Yang, L. Ci, J. A. Bur, S.-Y. Lin, and P. M. Ajayan, Nano Lett. **8**(2), 446 (2008).
[19]Y.-S. Chen, W. Frey, S. Kim, P. Kruizinga, K. Homan, and S. Emelianov, Nano Lett. **11**(2), 348 (2011).
[20]G. S. Kino, *Acoustic Waves: Devices, Imaging, and Analog Signal Processing* (Prentice-Hall, Englewood Cliffs, NJ, 1987).
[21]See supplementary material at http://dx.doi.org/10.1063/1.4934587 for detailed explanations.
[22]X. Zou, N. Wu, Y. Tian, and X. Wang, Opt. Express **22**(15), 18119 (2014).
[23]I. G. Calasso, W. Craig, and G. J. Diebold, Phys. Rev. Lett. **86**(16), 3550 (2001).
[24]G. Diebold, T. Sun, and M. Khan, Phys. Rev. Lett. **67**(24), 3384 (1991).
[25]G. C. Wetsel, Jr., IEEE Trans. Ultrason. Ferroelectr. Freq. Control **33**(5), 450 (1986).
[26]T. Lee, J. G. Ok, H. S. Youn, L. J. Guo, and H. W. Baac, in IEEE International Ultrasonics Symposium (IUS) (2014).